Flocculation of fiber suspensions studied by Rheo-OCT

ANTTI I. KOPONEN, JUAN CECCHINI, OLLI-VILLE LAUKKANEN, AND ARI JÄSBERG

ABSTRACT: When dealing with papermaking fiber suspensions, particle flocculation takes place even before the paper web is formed. The particle flocculation depends on several aspects, including particle mass concentration (consistency), particle collisions, electrochemical interactions promoted by chemical additives, etc. Due to its importance, fiber suspension flocculation has been studied for a long time in papermaking, and several methods have been developed for this purpose. The traditional techniques include, for example, focused beam reflectance microscopy (FBRM) and high-speed video imaging (HSVI).

Recently, a new optical method, optical coherence tomography (OCT), has emerged for flocculation analysis. The advantages of OCT are the possibility to study opaque suspensions, its micron-level resolution, and its high data acquisition speed. The OCT measurements can be combined with rheological (Rheo) measurements, allowing simultaneous measurement of both the time evolution of the floc size and the suspension viscosity.

In this work, we used this approach, Rheo-OCT, to study the flocculation of suspensions of various papermaking furnishes. We analyzed the time evolution of the floc size and the fiber suspension viscosity when the studied papermaking suspensions were treated with highly refined furnish (HRF) — a furnish that contained a significant amount of micofibrillated cellulose (MFC)-type fibrils — and/or chemical additives. Such studies can lead to a better understanding of the impact of flocculation on the produced paper web in terms of qualities like formation, drainage potential, and strength behavior.

Application: Readers of this research can use the results to improve their understanding of fiber suspension flocculation in papermaking and learn about a new method, Rheo-OCT, that can be used in such studies. In addition, the insights gained in this study regarding the effect of HRF and chemical additives on flocculation can lead to improvements in paper formation, drainage potential, and strength properties.

In recent years, when developing better printing and writing paper quality grades, the papermaking industry has been pressured to improve the quality and uniformity of their products, particularly formation, smoothness, and printability. Currently, there is a growing demand for enhanced paperboard quality, particularly for the case of test linerboard and fluting (TL&F) and folding box board (FBB) based packaging. This necessitates a focus on strengthening the boards (especially internal bond) while ensuring minimal compromise on finishing performance.

It is well known that the paper and board structure and strength performance depend, at least to some extent, on the characteristics of the flocculated components. At the macroscale, the strength responses can depend on generic factors (furnish component characteristics, forming technologies, etc.), while microscale factors (fines particles retention, flocculation characteristics, etc.) can contribute to the strength development through their bonding characteristics and networking responses.

As lightweight paper and board grades are continually developed to serve diverse purposes, optimizing the use of specific furnishes and their components, coupled with tailored treatments, has become increasingly important. Characterizing particle interactions within papermaking suspension is essential for developing effective methods to enhance the utilization of a given furnish and achieve desired properties in the final product. Particle sizes and chemistry play a significant role in this context.

Studying particle flocculation can clarify how specific microscale conformations influence the macroscale formation of paper and board structures. This paper provides a novel measurement method for this purpose based on a combination of optical coherence tomography (OCT) and a rheometer (Rheo) for measuring particle flocculation that is called Rheo-OCT. We used this method to analyze the time evolution of the floc size and the fiber suspension viscosity when the studied papermaking suspensions were treated with highly refined furnish (HRF) — a furnish that contained a significant amount of micofibrillated cellulose (MFC)-type fibrils — and/or chemical additives.

BASIC CONCEPTS OF FLOCCULATION

"Aggregation" and "flocculation" both refer to the formation of particle clusters in a suspension, and these terms are often used interchangeably. However, they have slightly different meanings: Aggregation refers to any process where particles form clusters (or aggregates), while flocculation usually describes a process where flocculants are used to enhance aggregation. In this paper, we have

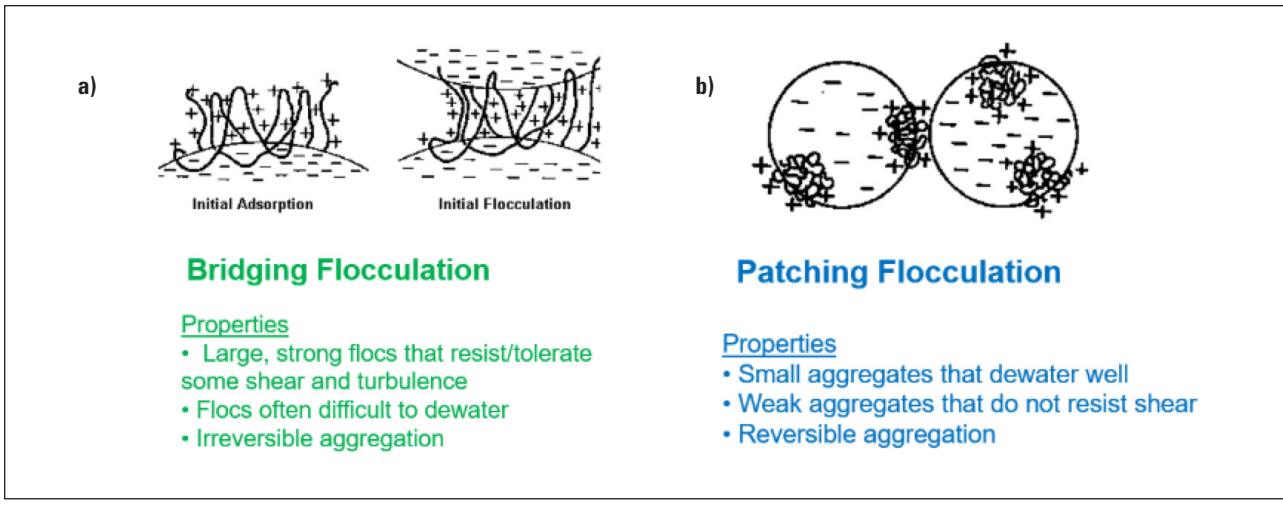

1. Chemical additives cause fine particle flocculation by either (a) bridging or (b) patching [3].

chosen to consistently use the term "flocculation," because we are studying the effect of flocculants on aggregation in papermaking stocks.

In papermaking fiber suspensions, particle flocculation takes place even before the paper web is formed. Several different factors affect particle flocculation, including particle (mass) concentration (consistency), particle collisions, electrochemical interactions promoted by chemical additives, and more. Because of its importance, the flocculation of fiber suspensions has been a widely studied topic in the paper industry.

The most relevant fundamental aspects of flocculation are highlighted in Blanco et al. [1], who describe the basic interactions taking place in a papermaking fiber suspension. Mechanical and electrochemical interactions play a central role in floc formation. The relative strength of various interactions is affected by the particle size (fibers, fibrils, fines, fillers, chemical additives, etc.) and the scale and geometry of the macroscopic environment (pumps, screens, pipes, valves, etc.) where the fiber suspension is processed. The particle size and concentration determine the collision probability in a given fluidization regime, while the mechanical elements (devices) will dictate the flow conditions (shear forces, fractionations, etc.) affecting the contact time between interacting particles. The microscopic and macroscopic conditions together define the flocculation characteristics of a given element of a papermaking suspension.

Many quantities can affect the way the particles flocculate. For example, the crowding number, defined as the average number of fibers in the volume swept by a single fiber [2], has been widely used to describe the flocculation (and formation) potential of furnishes. The crowding number decreases, for example, with decreasing fiber length or fiber consistency; simultaneously, the floc size typically decreases, and the formation of paper improves. One can speculate that decreasing floc size leads to smaller pore size, providing a potential advantage in terms of improved dewatering after the waterline and increased dry solids contents in the formed wet web. However, the crowding number is purely a statistical factor, and it does not account for the flocculation tendency caused, for example, by the variable chemical environment in which the fibers are embedded and the shear forces acting on the flocs from the approach flow to the headbox and forming section subprocesses.

Chemical additives play a significant role in flocculation. They affect the flocculation of fine particles through electrochemical interactions that depend, for example, on the molecular weight of the polyelectrolyte (polymer) used and the charge densities of the components. When high molecular weight additives are involved, the particle interaction mechanism is mostly bridging, while the medium molecular weight additives cause patching flocculation (**Fig. 1**) [3]. Disruptions in bridging flocculation are irreversible, whereas disruptions in patch flocculation are reversible. Another potentially important parameter is the specific surface area (SSA) of the particles.

EXAMPLES OF FLOCCULATION MEASUREMENT TECHNIQUES

There are numerous methods available for studying particle flocculation. On a laboratory scale, most of these methods are quite straightforward to use, while inline analysis of industrial processes is often feasible with proper prearrangements. Various methods are discussed in detail by Rasteiro and Koponen [4]. Here, we present four earlier examples of how particle flocculation has been measured in the past to evaluate the wood fiber flocculation. In the next section, we introduce a new method, optical coherence tomography (OCT), which can also be used for this purpose.

By the end of the 1990s, advancements in high-speed cameras allowed their application for wood fiber flocculation studies. Flocculation was studied in various flow geometries both on laboratory scale and pilot scale. Generally, the

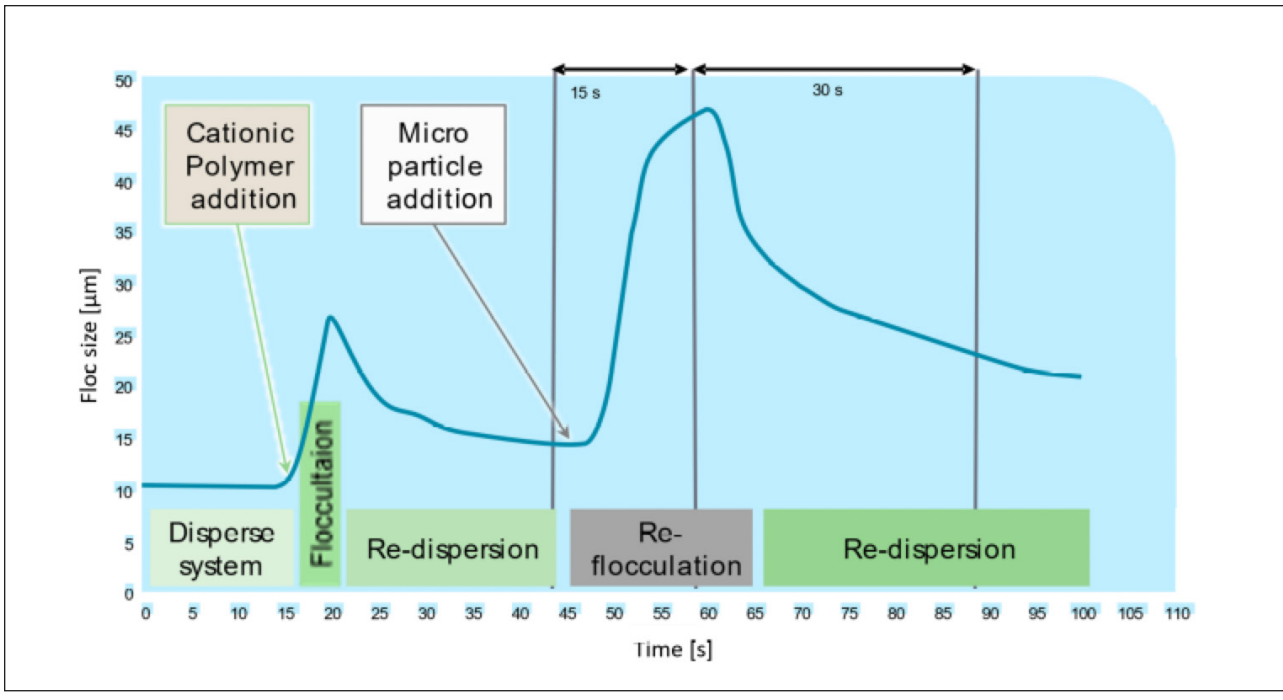

2. An example of a focused beam reflectance microscopy (FBRM) flocculation dynamics curve in a beaker during mixing for a certain papermaking suspension under the effects of cationic polymer and subsequent microparticle additions (based on data from [7]).

resolution of such studies is not as high as, for example, focused beam reflectance microscopy (FBRM) that is discussed later, but with proper optics, micrometer accuracy can also obtained. As an example, Kellomäki et al. [5] used transillumination to study flocculation in concentric pipe constructions with different flow rates. The motivation for such study was to optimize the headbox geometry to obtain a good formation of the final product [6].

The FBRM technique was introduced in the 1990s in the mining industry. It is based on a submerged monitoring device that utilizes a rotating laser beam to sweep over the particles in the suspension. The light backscattered from the particles is used for the floc size analysis. The resolution of FBRM is high, on the micrometer scale. In the early 2000s, FBRM was introduced for studying the flocculation of papermaking suspension particles, such as fiber fines and fillers [7,8]. Here, the emphasis was particularly on the effects of chemical additives on particle-particle interactions. These studies revealed that when various chemical additives were applied to different fiber suspensions (including a wide range of particle sizes), characteristic responses called flocculation dynamics curves were obtained, as demonstrated in **Fig. 2**.

The photometric dispersion analyzer (PDA), developed in the 1980s [9], is a non-invasive technique for measuring the size of particles in a suspension with micrometer resolution in real time. Here, a beam of light is passed through a sample, and the intensity of transmitted light and its fluctuations are used to calculate the particle size. In [10], PDA was successfully used to analyze the floc size of a typical papermaking furnish treated with a two-component microparticle retention system under various shear rate conditions.

The suspension flocculation can also be indirectly studied by analyzing the viscous behavior of the suspension. The simplest way to do this is to measure the time evolution of torque acting on a rotating rotor during an experiment. This approach has been used successfully for identifying optimal polymer solutions with a wide variety of furnishes in real-life applications [11]. Note that in this paper, we use this approach by performing the experiments in a rheometer.

OPTICAL COHERENCE TOMOGRAPHY

Optical coherence tomography (OCT) [12,13] is a recent optical measurement technique for flocculation analysis [14,15]. It employs low-coherence spectroscopy and interferometry to determine the optical properties of the studied sample as a one-dimensional (1D) depth-dependent reflectivity profile (A-scans). The two dimensional (2D) images (B-scans) or three dimensional (3D) volumes can be constructed from a series of A-scans at different lateral positions, as demonstrated in **Fig. 3**.

In the first realization of OCT, time-domain OCT (TD-OCT), light from a low-coherence source is split by a coupler into two paths: a reference arm and a sample arm, as shown in **Fig. 4** (left image). In the reference arm, light is back-reflected by a reference mirror and returns through the same path. In the sample arm, light is backscattered by the sample, with varying backscattering intensity depending on the

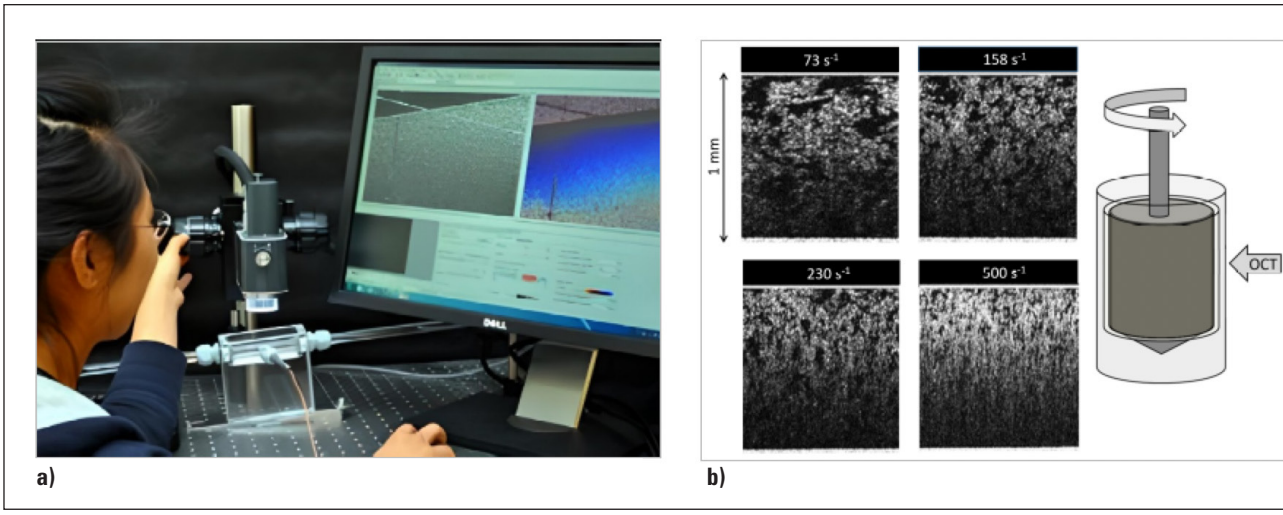

3. (a) Measurement of flow in a capillary with optical coherence tomography (OCT), and (b) two-dimensional (2D) structural OCT images of microfibrillated cellulose (MFC) with different shear rates in a concentric cylinder geometry [16].

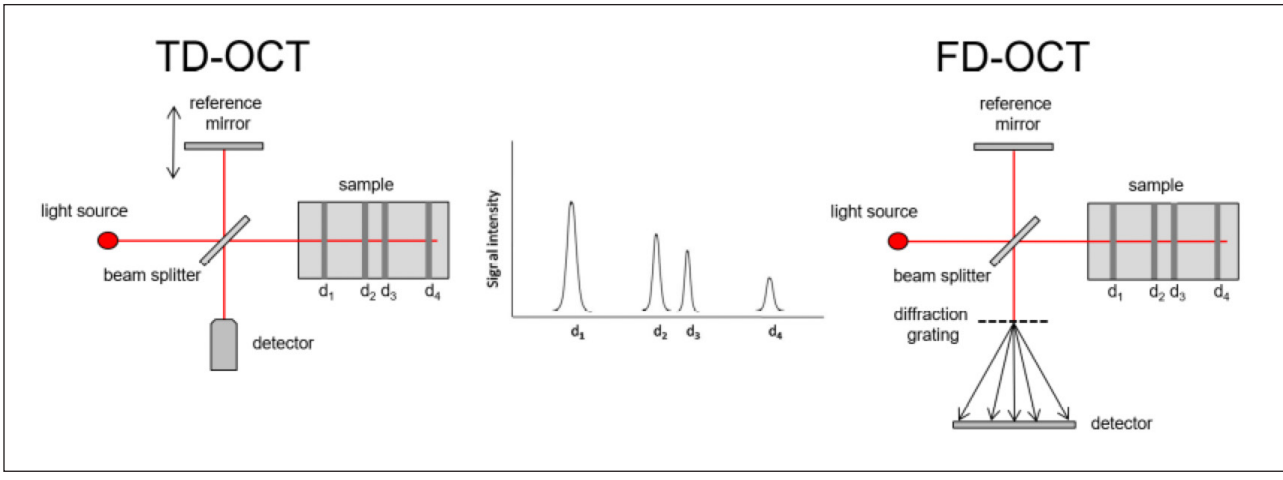

4. In time-domain OCT (TD-OCT), the reference mirror moves during the measurement, and the signal is obtained at a specific time from a specific location. The different interfaces of the sample lead to a spike in the interference level, which appears as a spike in the signal strength graph. In Fourier-domain OCT (FD-OCT), the reference mirror is fixed and the interferometer detector arm uses a spectrometer instead of a single detector. The spectrometer measures the spectral modulations resulting from the interference of the sample and reference reflections [13].

sample's internal structure. The returning light from both arms recombines at the coupler, generating an interference pattern recorded by the detector. As the reference mirror moves, it generates interference patterns with light backscattered from corresponding depths within the sample, allowing for the measurement of light backscattered from different depths beneath the sample surface.

In the Fourier (or spectral) domain OCT (FD-OCT) used in this study, the light echoes are simultaneously collected from all axial depths and observed as modulations of the source spectrum, thus capturing all spectral components at once, as shown in Fig. 4 (right image). This technique is called Fourier domain OCT because the interference pattern is recorded in the spectral domain for each lateral position, and the final image is reconstructed by the Fourier transform. The main difference between FD-OCT and TD-OCT is that in FD-OCT, the reference mirror is static, unlike the moving mirror used in TD-OCT. This feature removes the moving mirror and the associated limitations caused by its mechanical inertia. Consequently, FD-OCT systems achieve significantly faster data acquisition rates than TD-OCT systems.

A significant advantage of OCT is the possibility to use it for the analysis of opaque suspensions. The resolution of OCT is on the micrometer scale, and the data acquisition speed is in the tens or even hundreds of kilohertz. Imaging depth depends strongly on the studied medium but is typically on the order of one millimeter. If optical access can be arranged, OCT can be applied to various flow geometries such as capillaries, pipes, and rheometer geometries. This measurement concept, called Rheo-OCT, was used in this study.

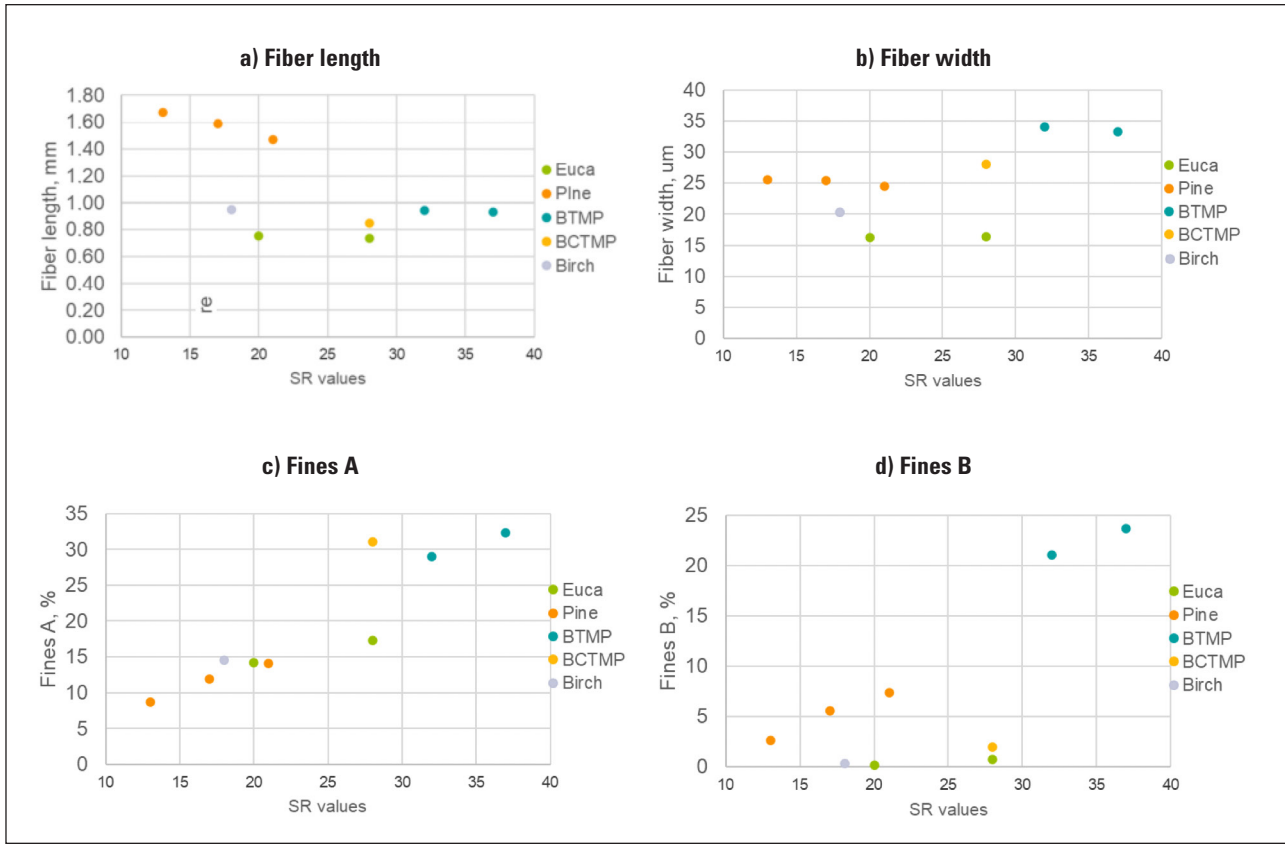

5. Example of characteristics of various folding boxboard (FBB) stock components, including eucalyptus (Euca) bleached kraft pulp (BKP); pine BKP; bleached thermomechanical pulp (BTMP); bleached chemithermomechanical pulp (BCTMP); and birch BKP as a function of drainability (SR value): (a) fiber length, (b) fiber width, (c) Fines A percentage (flake-like fines), and (d) Fines B percentage (fibril-like fines). The measurements were performed with the Valmet FS5 Fiber Analyzer.

MATERIALS AND METHODS

Furnishes

In most cases, the outer plies (top and back) of FBB are produced by a combination of hardwood bleached kraft pulp (HWBKP) and softwood bleached kraft pulp (SWBKP). The filler ply is produced with a combination of mechanical-based pulp such as bleached chemithermomechanical pulp (BCTMP), bleached thermomechanical pulp (BTMP), or chemithermomechanical (CTMP); a portion of bleached kraft pulp (BKP); and, normally, a certain amount of broke (coated and uncoated). The typical characteristics of various FBB stock components, measured with the Valmet FS5 fiber analyzer (Valmet; Espoo, Finland), are shown in **Fig. 5**.

The furnish components of the studied stocks were according to the approximate standard mix for FBB filler ply, namely BKP (HW/SW), mechanical pulp (BCTMP), and broke in variable proportions. The average refining degree (drainability) of the furnish components was 25–30 SR.

For three stocks, we used an HRF as the reinforcement stock. The HRF contains a certain amount of MFC-type material (e.g., fibrils). It was produced from SWBKP by a double-disc (DD) refiner operated in batch conditions with a heat exchanger included in the process. This was achieved by performing the first two refining passes with cutting fiber fillings, while the rest of the refining was done with fibrillation fiber fillings. The refining led to a drop in the average fiber length from ~1.6 to ~0.7 mm, while the Fines A and Fines B content (flakes- and fibrils-type elements) changed from 16% to 37% for Fines A, and from 3% to 62% for Fines B, as shown in **Fig. 6**.

Chemical additives

One can find in the literature numerous combinations of chemical additives that can be used for different reinforcement purposes. The additives used in this study were selected based on specific customer needs, and to limit the scope of the study, we excluded other flocculants, such as polyacrylamide, despite their importance. The observed responses are thus based on a limited number of chemical additives. The following chemical additives were chosen:

- Cationic starch: Raisamyl 70021 (DS 0.042) from Chemigate (Lapua, Finland)
- Polyaluminum chloride (PAC): PAX-XL19 from Kemira (Helsinki, Finland)

Cationic starch is expected to primarily promote bridging flocculation. Cationic PAC is a fixative/coagulant that has a high positive charge density, which allows it to neutralize the negative charges on fines and fibrils, promoting

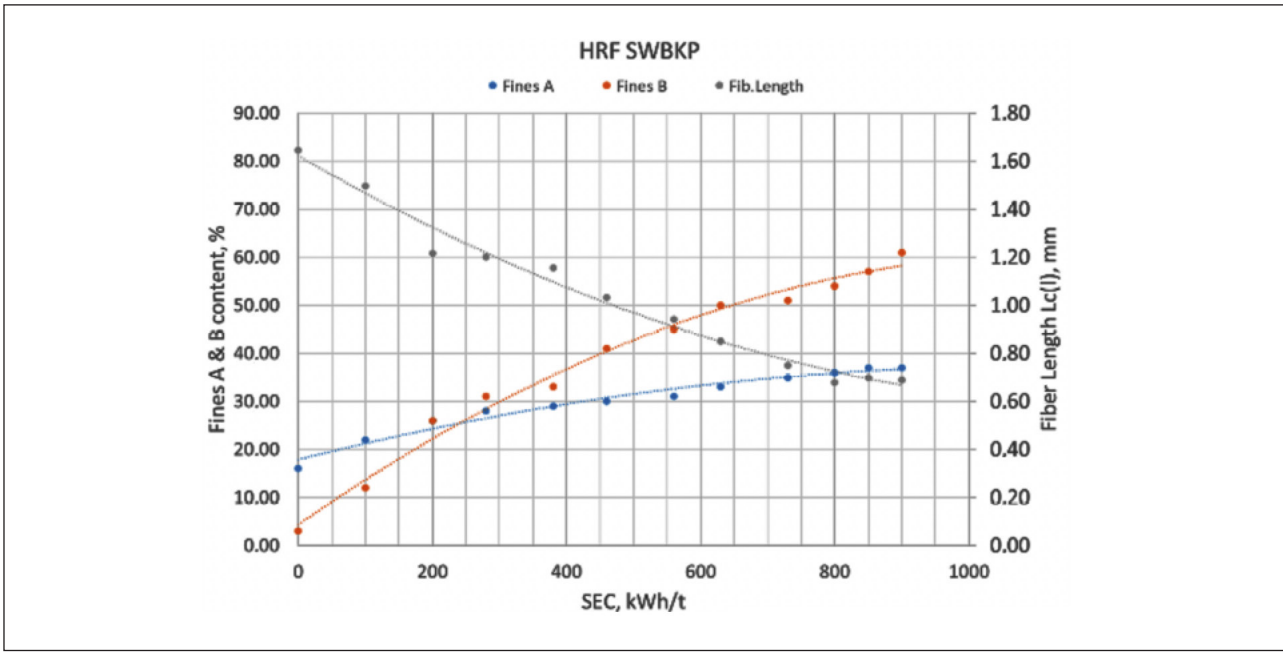

6. Highly refined furnish (HRF) softwood bleached kraft pulp (SWBKP) development with refining. The graph includes the average fiber length and Fines A and B percentages as a function of specific refining energy consumption (SEC). The measurements have been performed with the Valmet FS5 Fiber Analyzer.

flocculation. While PAC's molecular size is too small to effectively promote patching flocculation in the main stock, it does induce patching flocculation in smaller fines and fibrils. The microparticle, chosen for the real-life application, was colloidal silica due to its well-known impact as a drainage agent and its high reactivity with cationic starch and/or highly cationic-charged synthetic polymers. Its effect on flocculation was not studied in this work.

Selection of HRF treatment dosages with chemical additives

Since the MFC fibril-like particles in HRF have a significantly high SSA, it was deemed convenient to test them with similar dosages to those used in conventional papermaking stock additions. It is common to apply 4, 8, or 12 kg/metric ton of cationic starch to a papermaking stock in the wet end. These dosages represent a 0.4%, 0.8%, or 1.2% chemical addition.

When adding reinforcement stocks like SWBKP to base papermaking furnishes, dosages typically range from 5% to 20% with moderate-to-low refining conditions. For HRF, since it could negatively affect dewatering, the dosage is usually dropped to 3%–7% due to the higher amount of fines. The high concentration of fines in HRF could potentially lead to poor first-pass retention; thus, HRF will require a higher dosage of retention aid and a greater amount of drainage agent to help control retention and dewatering. The high specific surface area of HRF requires a relatively large amount of retention aid. To address this challenge, preaggregation of HRF could improve retention efficiency, allowing for the use of more moderate dosages of the retention aid.

Due to the previously-mentioned reasons, in HRF flocculation tests, HRF particles were treated with significant amounts of cationic starch, specifically 40 or 80 kg/metric ton. While such dosage might be considered excessive, it is important to remember that the chemically treated HRF will be used as a reinforcement pulp in a base papermaking stock, and it is necessary to determine the actual ratio of additive to be fed in the final mix. When adding 5% of HRF with 80 kg/metric ton (8%) of cationic starch, we are adding 0.4% (50 kg/metric ton × 0.08 = 4 kg/metric ton) starch to the main stock. Thus, if the original dosage of starch was, for example, 8 kg/metric ton, we are saving 4 kg/metric ton of cationic starch in the base papermaking stock treatment.

Rheo-OCT: Optical coherence tomography combined with a rheometer

The OCT measurements were performed using Telesto I SD-OCT (Thorlabs; Newton, NJ, USA) in the vicinity of the wall of a rheometer cup. The system's depth pixel resolution is 3.7 µm in water. The scanning rates were 25 and 91 kHz. The OCT was employed to record structural images of the suspensions while they were sheared in a vane-in-cup geometry of a rotational rheometer. Images of the measurement geometry are shown in **Fig. 7**. During the OCT measurements, the time evolution of suspension viscosity was measured with the rheometer as detailed below.

The original OCT images consisted of a long series of radial B-scans (of the order of one million A-scans). The

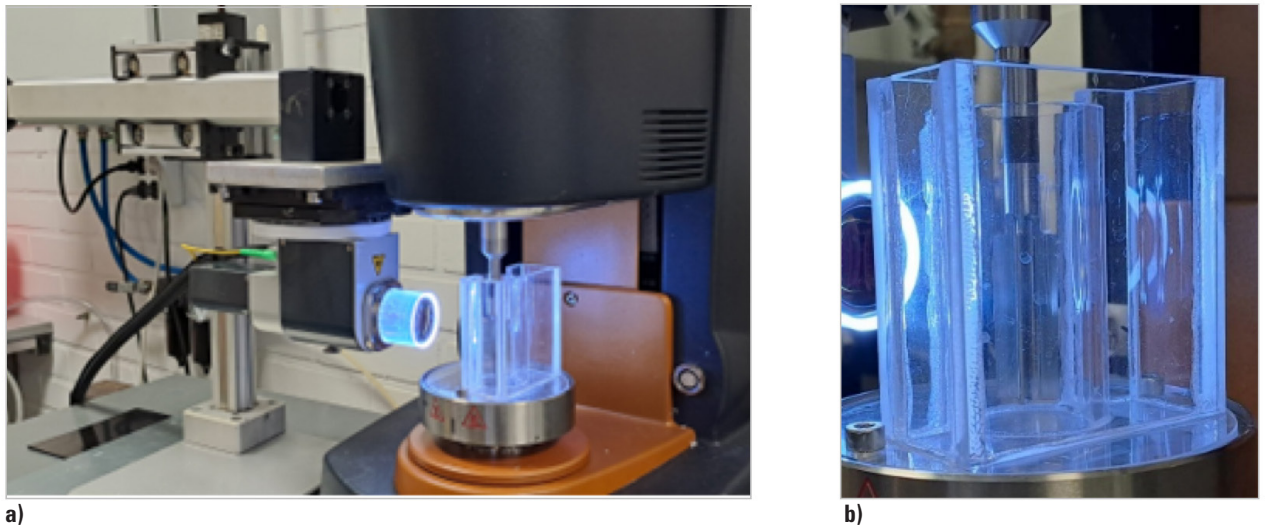

7. (a) The Rheo-OCT measurement setup used in this study, and (b) the transparent cylinder geometry together with the vane used in this study. Notice that the cylindrical cup is surrounded by pools that can be filled with water. These pools are incorporated to enhance optical matching for certain imaging setups. They were not used in this study.

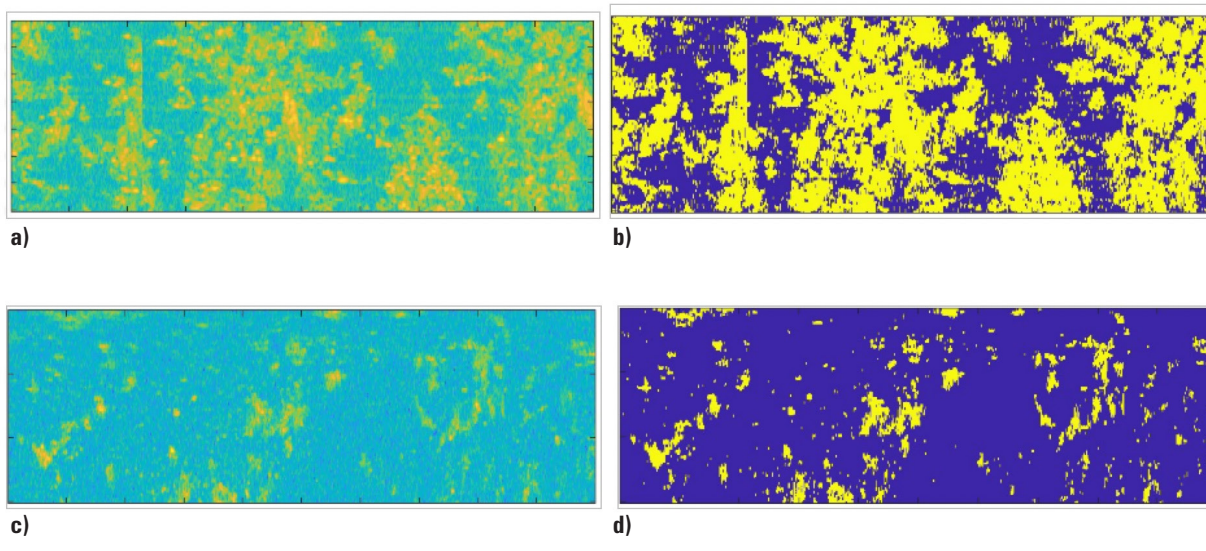

8. A median filtered structural OCT image of (a) an HRF fiber suspension, and (c) a papermaking furnish suspension, with (b) and (d) corresponding binarized OCT images. The image height is 0.5 mm, and the width is 2.5 mm. The cup wall is close to the upper boundary of the images.

OCT measurement depth was limited to about 500 µm from the cup wall due to the rapid increase in noise levels when probing deeper into the suspension. The OCT floc size analysis was as follows: The depth-dependent decay of the OCT signal was first corrected by calculating the average OCT signal as a function of depth and then scaling the pixel values at each depth accordingly. Next, the noise level of the images was decreased by filtering them in the radial direction using a 3 × 1 median filter (**Fig. 8a** and Fig. 8c). The images were then binarized to divide the images into the solid phase and water phase (Fig. 8b and Fig. 8d). For the HRF suspensions, the binarizing threshold was set to 1.0, and for the papermaking stocks, it was set to 1.2. Finally, the radial floc size distributions were calculated as run-length distributions. The image analysis is explained in detail in Lauri et al. [15].

Figure 9 shows an example of the OCT floc analysis with two shear rates for 0.5% Celish MFC (Daicel; Osaka, Japan) that has been treated with cationic polyacrylamide (cPAM). As shown in Fig. 9, the floc size first increases significantly and then gradually decreases due to shear forces breaking the flocs into smaller pieces.

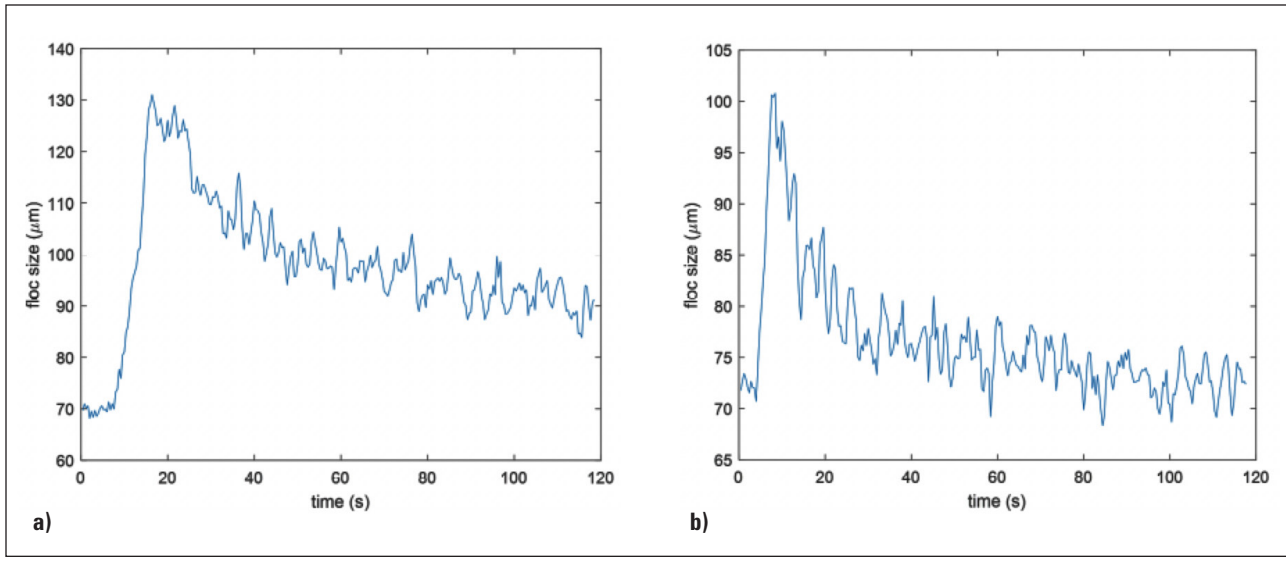

9. Time evolution of flocculation of 0.5% Celish MFC that has been treated with cationic polyacrylamide (cPAM). The shear rate is (a) 120 s^{-1} and (b) 200 s^{-1}. The additive has been added at t *= 5 s.*

Simultaneously with OCT imaging, the (apparent) viscosities of the suspensions were measured using a stress-controlled TA Instruments DHR-2 rheometer (TA Instruments; New Castle, DE, USA) using a vane-in-cup geometry (Fig. 7). The diameter of the four-blade vane was 15 mm, and the inner diameter of the transparent cup was 30 mm, resulting in an effective measurement gap of 7.5 mm. The use of such a wide-gap vane geometry minimizes possible wall slip effects [17] and avoids confinement effects that would be caused by the comparable size of the flocs and the measurement gap [18]. However, it should be noted that this measurement geometry is not optimized for measuring the viscosity of low-viscosity liquids at high shear rates due to the potential generation of secondary flows between the blades of the vane [19]. Thus, the viscosity values reported in this paper are apparent and may not be fully accurate in terms of absolute values. Additionally, notice that the small-gap approximation, typically applicable for standard rheometer geometries like concentric cylinders or cone-and-plate setups, does not hold for the wide-gap vane-in-cup geometry. Therefore, the shear rate is not uniform throughout the gap or inside the sample [20], and it is more accurate to refer to the shear rate as an apparent shear rate.

The additives were always manually injected at a single point near the cup wall. Testing with a colored additive solution confirmed that the additives dispersed throughout the entire cup within a few seconds. As an additional technical note, the vane geometry was positioned close to the bottom of the cup (the vertical gap between the lower edge of the vane and the bottom of the cup was 1 mm) to mitigate the sedimentation of fibers during the measurements. This positioning may have introduced additional systematic error in the measured viscosity values due to end effects [21]. However, since this paper focuses on analyzing relative changes in viscosity and their timescales during fiber flocculation and deflocculation, rather than comparing absolute viscosity values, these potential experimental artefacts do not impact the conclusions. To improve the accuracy of the viscosity measurements and to create a more axisymmetric shear stress and shear rate field, serrated concentric cylinders or fractal vane geometries [21] could be employed in future studies on this topic.

Determining an appropriate shear rate for the measurements

The optimal shear rate for the flocculation measurement was determined by adding a flocculant to the studied fiber suspensions and gradually increasing the shear rate (**Fig. 10**). Due to shear thinning, viscosity decreased with an increasing shear rate, but it remained constant as a function of time at a fixed shear rate until the shear rate was high enough to start breaking the flocs. The breakdown of the flocs manifests itself as a decrease in viscosity with time at a constant shear rate, as is observed to occur at a shear rate of $\dot{\gamma}$ = 80 s^{-1} for the HRF furnish and additive studied in Fig. 10. For the papermaking furnishes, this shear rate was $\dot{\gamma}$ = 55 s^{-1}. These shear rates were used for the actual flocculation studies. Note that the optimal shear rate for these kinds of flocculation/deflocculation studies depends on the type of furnish and flocculant used. The shear rate scan measurement can thus be used to estimate the strength of the flocs; strongly bound flocs require a higher shear rate to be broken down than weakly bound flocs. **Figure 11** illustrates the time evolution of viscosity and floc size for refined SWBKP furnish after successive addition of starch, anionic polyacrylamide (aPAM), and micropolymer.

The vane-in-cup geometry is more sensitive to secondary

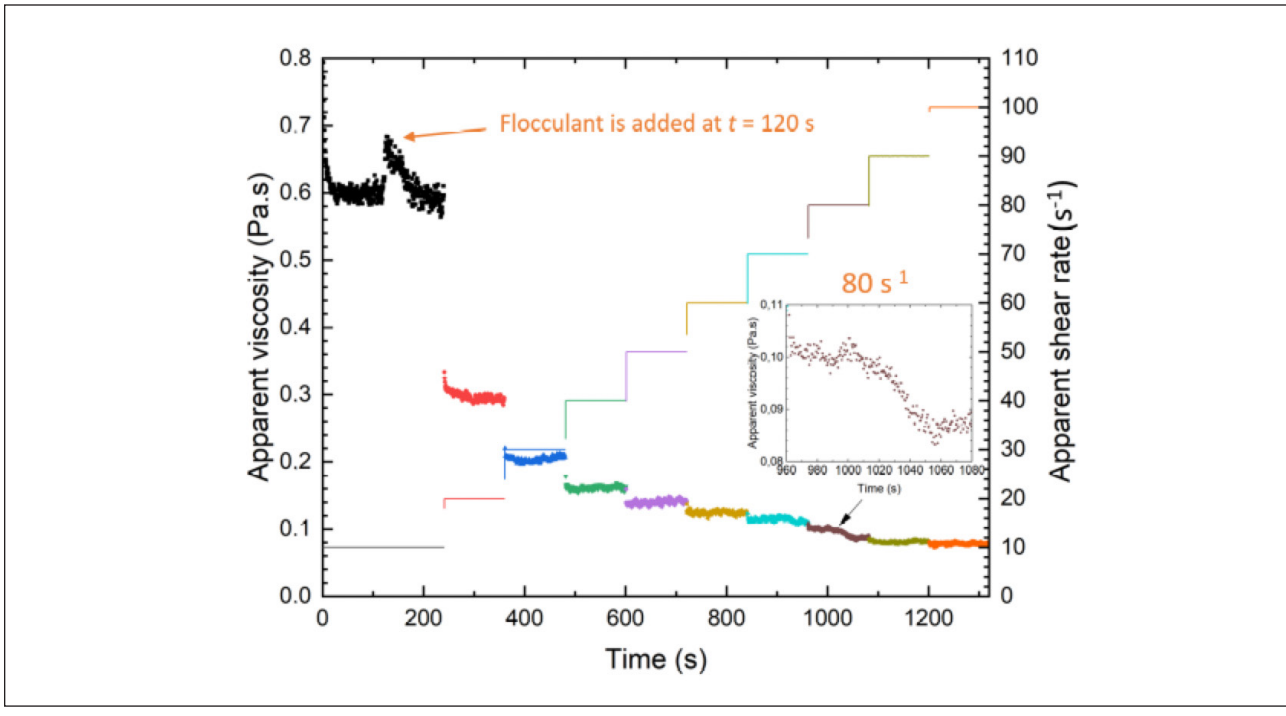

10. Determining shear rate (80 s^{-1}) that was used in the flocculation studies of the HRF furnish.

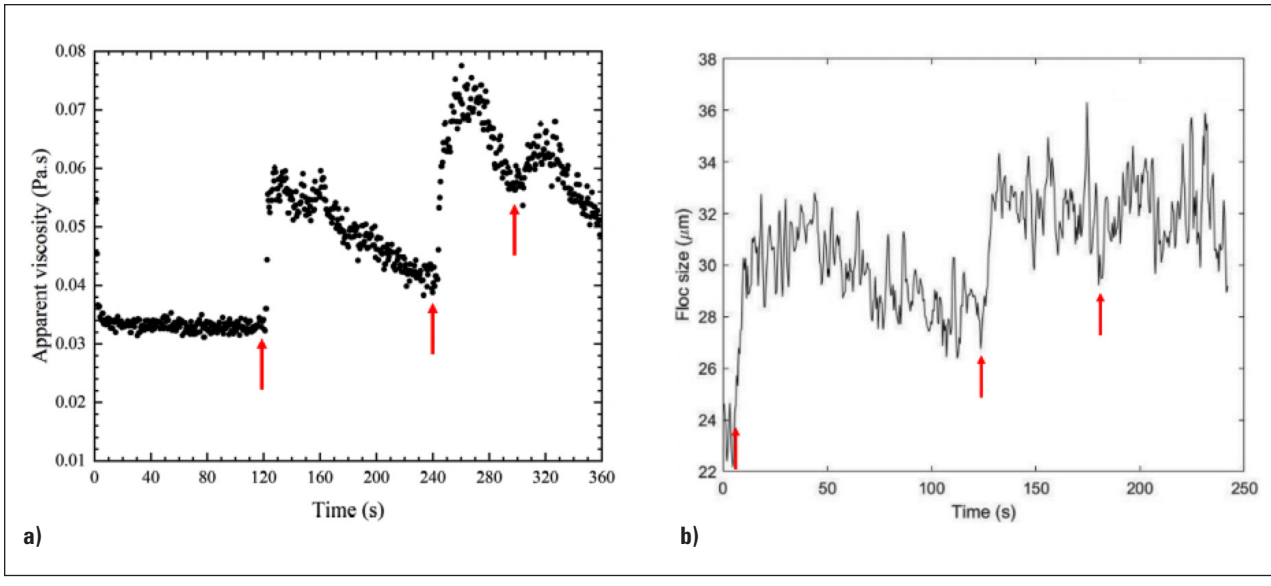

11. The time evolution of (a) viscosity and (b) floc size for refined SWBKP furnish after successive addition of starch, anionic polyacrylamide (aPAM), and micropolymer. (The shear rate is 55 s^{-1}. The dosage times are shown with red arrows.)

flows compared to traditional rheometer geometries, such as plate-plate or concentric cylinder setups. The Reynolds number for Couette concentric-cylinder systems is defined as [22]:

$$\mathrm{Re} = \frac{\Omega R_i R_o (1 - 1/\delta)\rho}{\mu_N} \quad (1)$$

where Ω is the angular velocity of the vane; R_i is the radius of the vane; R_o is the cup radius; $\delta = R_o/R_i$; ρ is the suspension density; and μ_N is the nominal (here apparent) viscosity of the suspensions. The strain constant was $K_\gamma = (1 + \delta^2)/(\delta^2 - 1) = \dot{\gamma}/\Omega = 1.666$. The Reynolds number of HRF experiments was 49, whereas for the six stocks, it was less than 20. The critical Reynolds number for secondary flow is 54 according to Crawford, Sprague, and Stickel [22]. Moreover, as the viscosity of HRF followed a power law at

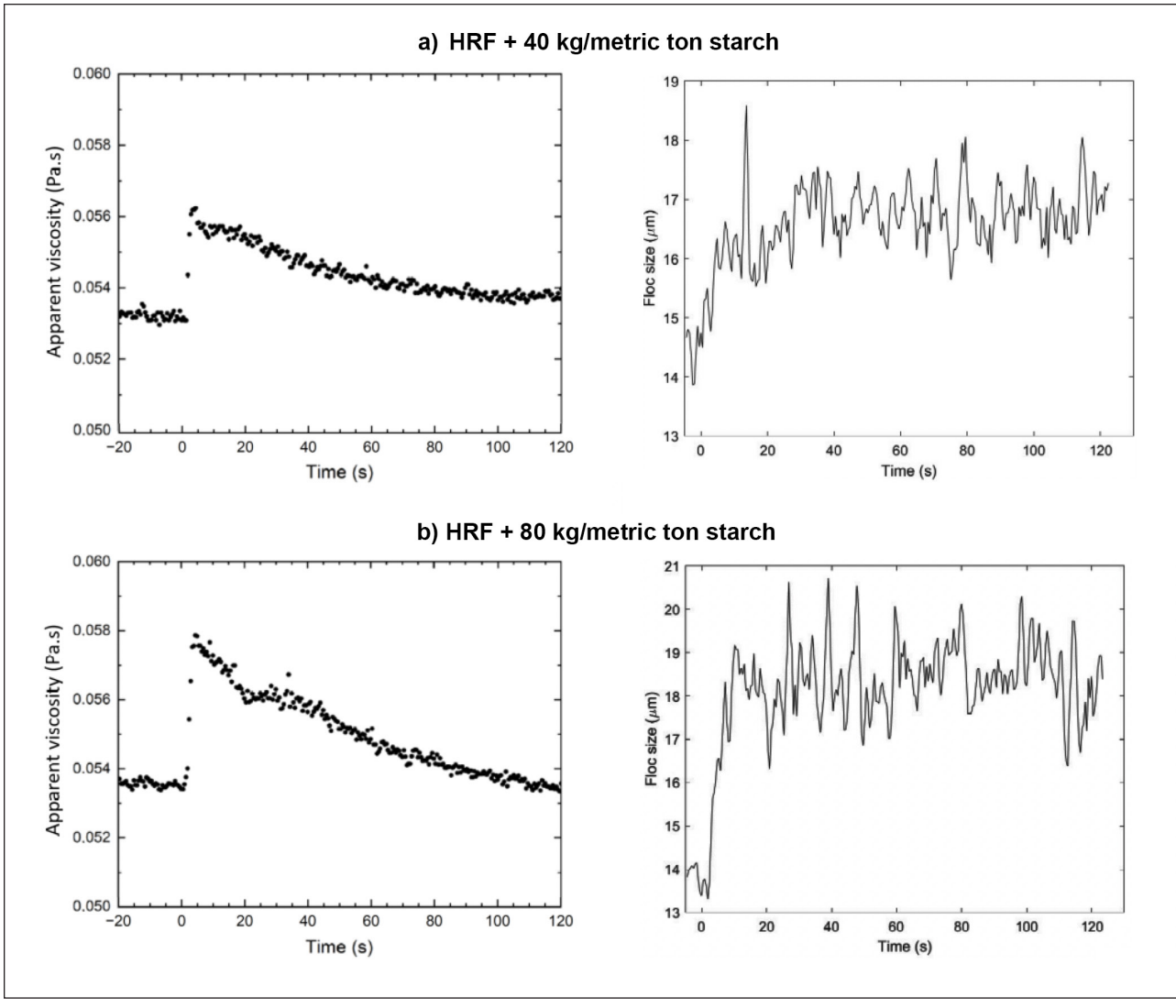

12. Flocculation and viscosity responses of 0.5% HRF treated with two dosages of cationic starch under the same shear rate conditions (80 s^{-1}): (a) 40 kg/metric ton starch, and (b) 80 kg/metric ton starch. Notice that here and in Figs.13–15, the additive has been added at t *= 0 s.*

least up to the shear rate 100 s^{-1} (as shown in Fig. 10), the effect of secondary flows was likely negligible in these measurements.

RESULTS

Flocculation and viscosity tests with HRF suspension treated with cationic starch

The Rheo-OCT experiments with the HRF suspension were performed at 0.5% consistency. The shear rate in these measurements was 80 s^{-1}. **Figure 12** shows both the time evolution of the viscosity and the floc size after adding either 40 or 80 kg/metric ton of starch to the HRF. As seen in Fig. 12, the responses are qualitatively similar, while the effect is slightly stronger for the higher dosage. Note that the viscosity first increases rapidly and then gradually decreases. In contrast, the floc size rises rapidly, but remains constant after that. This can be explained as follows: In a vane-in-cup geometry, shear stress is highest at the outer edges of the vane and decreases towards the cup wall [23]. The floc structure near the vane dominates the rheometer viscosity measurements, and the strong shear forces near the vane eventually break the flocs into smaller pieces [15]. The OCT measurement, on the other hand, is performed close to the cup wall where the shear forces are much lower.

Flocculation and viscosity tests of HRF with PAC

Figure 13 shows both the time evolution of the viscosity and the floc size after adding either 40 or 80 kg/metric ton of PAC to the HRF. Compared to the addition of starch, the response in viscosity is minimal, while the floc size behaves similarly but is clearly lower. For the higher PAC dosage, the floc size is even slightly lower. This could be explained as follows: With the higher dosage of PAC, the increased

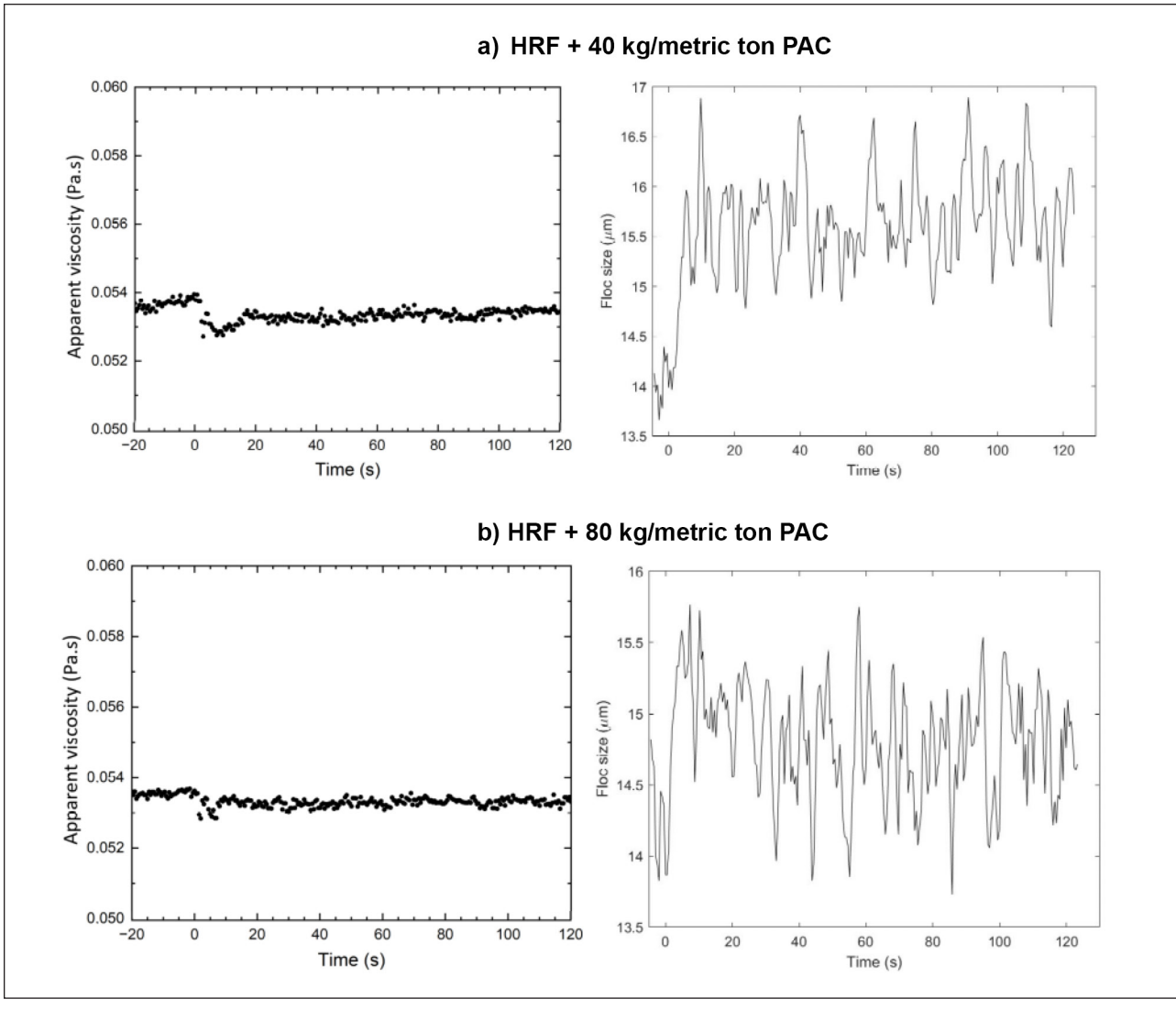

13. Flocculation responses and corresponding viscosity changes of 0.5% HRF with two dosages of polyaluminum chloride (PAC) under the same shear force conditions (80 s^{-1}): (a) 40 kg/metric ton PAC, and (b) 80 kg/metric ton PAC.

number of cationic patches formed on the particle surfaces might counteract flocculation to some extent. The minimal effect on viscosity can be attributed to PAC creating relatively weak, elongated particles that align along the shear field, thereby minimizing their impact on viscosity and leading to eventual breakage.

Flocculation tests with whole stock mixes

As discussed previously, individually treated HRF stocks showed an increase in floc sizes both with the addition of starch and PAC, though the effect was more pronounced with starch. Next, we will add either starch or HRF suspension pretreated with PAC to the base paper stock suspension to observe potential benefits in stock or additive savings. The studied pulps included variable amounts of BCTMP, HWBKP, SWBKP, and broke. The compositions of the studied stocks and the added amounts of HRF and additives are shown in **Table I**. The goal was to modify the stock composition to identify a more cost-effective mix that still responds adequately to flocculation additives.

Figure 14 shows a comparison between three base paper stocks with 20% BCTMP, 20% broke, and varying amounts of HWBKP (short and cheaper fibers) and SWBKP (long and expensive fibers), described as Stocks 1–3 in Table I. The comparison was done to determine the flocculation performance obtained with each stock combination when 8 kg/metric ton of cationic starch was added. As seen in Fig. 14, floc size evolution shows notable trend differences; the dwell time from the flocculant injection to the peak floc size is t = 20, 50, and 70 s for Stocks 1, 2, and 3, respectively. Thus, dwell time increases with a higher amount of HWBKP. Since dwell time varies between different furnishes, it is not only related to the dispersion of the flocculant but also to the reaction kinetics. The maximum floc size varies slightly across different stocks, and after reaching its peak, the floc size either remains almost constant or decreases slowly. The

Stock	BCTMP	Broke	SWBKP	HWBKP	HRF	Additive
1	20%	20%	20%	40%	0%	8 kg/metric ton starch
2	20%	20%	10%	50%	0%	8 kg/metric ton starch
3	20%	20%	0%	60%	0%	8 kg/metric ton starch
4	20%	20%	0%	55%	5%	2 kg/metric ton PAC
5	30%	20%	0%	45%	5%	2 kg/metric ton PAC
6	40%	20%	0%	35%	5%	2 kg/metric ton PAC

BCTMP: bleached chemithermomechanical pulp; SWBKP: softwood bleached kraft pulp; HWBKP: hardwood bleached kraft pulp; HRF: highly refined furnish; PAC: polyaluminum chloride.

I. The compositions of studied stocks and the added amounts of HRF and additives.

effect of the flocculant on viscosity is qualitatively similar in all three cases.

In **Fig. 15**, we compare base paper stocks with 20% broke and varying amounts of BCTMP (short, stiffer, and cheaper fibers) and HWBKP (short, flexible, and expensive fibers), described as Stocks 4–6 in Table I. The comparison was done to determine the flocculation performance obtained with each stock combination when 5% of HRF pretreated with 40 kg/ metric ton PAC was added. As seen in Fig. 15, the dwell time to the highest floc size is t = 20, 30, and 40 s for Stocks 4, 5, and 6, respectively. Dwell time thus increases with an increasing amount of BCTMP. The maximum floc size is similar across all three cases, and the floc size decreases monotonically after reaching its peak. The effect of the addition of the flocculant to viscosity is minimal, and viscosity gradually decreases by approximately 10% below the initial level.

DISCUSSION

Although the composition of Stocks 1–3 and Stocks 4–6 is different, we can make a few general observations of the stock flocculation dynamics, as demonstrated in **Fig. 16**. The highest obtained floc size is larger with starch. The dwell time to reach the highest floc size is longer with starch, but the floc size then remains approximately constant, whereas the flocs formed with HRF+PAC decrease gradually. This is due to starch causing bridging flocculation, which typically results in rather large flocs that have a good ability to maintain their size under shear forces [3]. On the other hand, when using HRF+PAC for reinforcement, the mixture should be added to the main stock close to the headbox to limit the time the formed flocs are exposed to disruptive shear forces. The addition of starch to the stock increases the viscosity temporarily (Fig. 14), whereas the effect of HRF+PAC on viscosity is negligible (Fig. 15). The dwell time to the highest floc size increases for both starch and HRF+PAC when the SSA of the furnish is increased (SWBKP replaced with HWBKP, or HWBKP replaced with BCTMP). These findings agree with earlier studies.

The chemical mechanism behind the stock flocculation caused by the combination of HRF+PAC is currently unclear. We present here a hypothesis that requires further studies: When solutions of oppositely charged polyelectrolytes are mixed, the resulting complexes can display an increased tendency to adsorb [24]. For instance, oppositely charged polyelectrolytes cPAM and aPAM are known to form complexes that, when pre-mixed before interacting with the furnish, can act as efficient flocculants and retention aids [25]. The PAC is a multivalent cation, and it will bind very strongly to multiple anionic sites on whatever it collides with in the papermaking furnish. A possible interpretation of the interactions between PAC and HRF is thus the potential for complexation. When PAC is added in excess to HRF, PAC might make the smallest fraction of HRF (i.e., the MFC fraction) cationic due to the fibril's high SSA. This process could then promote the aggregation of the remaining suspended particles. This interpretation suggests a novel perspective on furnish flocculation mechanisms, though it requires further investigation and more detailed measurement procedures than those discussed in this study.

When using flocculants, high flocculation indicates that the flocculating agent is effectively performing its role. Higher viscosity, larger floc size, and better stability of the floc size could then indicate that the stock mix can produce stronger flocs. This, in turn, could potentially result in a higher internal bond or higher relative bonded area of the final formed web. For papermakers, high flocculation may be a problem, as they typically prefer an unflocculated furnish to achieve high formation uniformity, which in turn helps improve the in-plane strength. However, the primary goal of this study was to increase the proportion of cost-effective furnishes in the filler ply of FBB. In this context, the most critical properties are bulk and internal bond, not the in-plane strength. One can speculate that both objectives might be achieved if shear forces are sufficient to break down the larger fiber flocs while preserving the attachments between fine particles and fibers.

a) Stock 1: BCTMP 20% + Broke 20% + SWBKP 20% + HWBKP 40% + 8 kg/metric ton starch

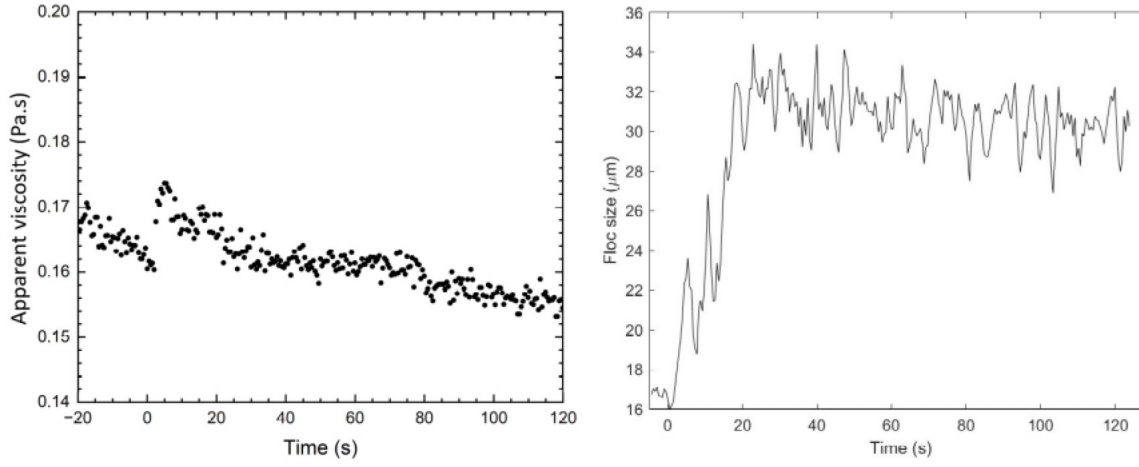

b) Stock 2: BCTMP 20% + Broke 20% + SWBKP 10% + HWBKP 50% + 8 kg/metric ton starch

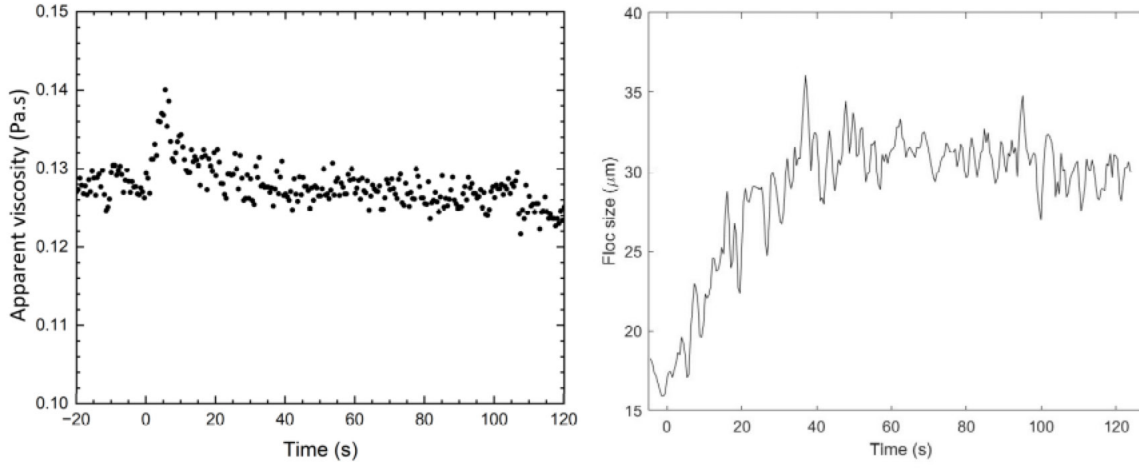

c) Stock 3: BCTMP 20% + Broke 20% + HWBKP 60% + 8 kg/metric ton starch

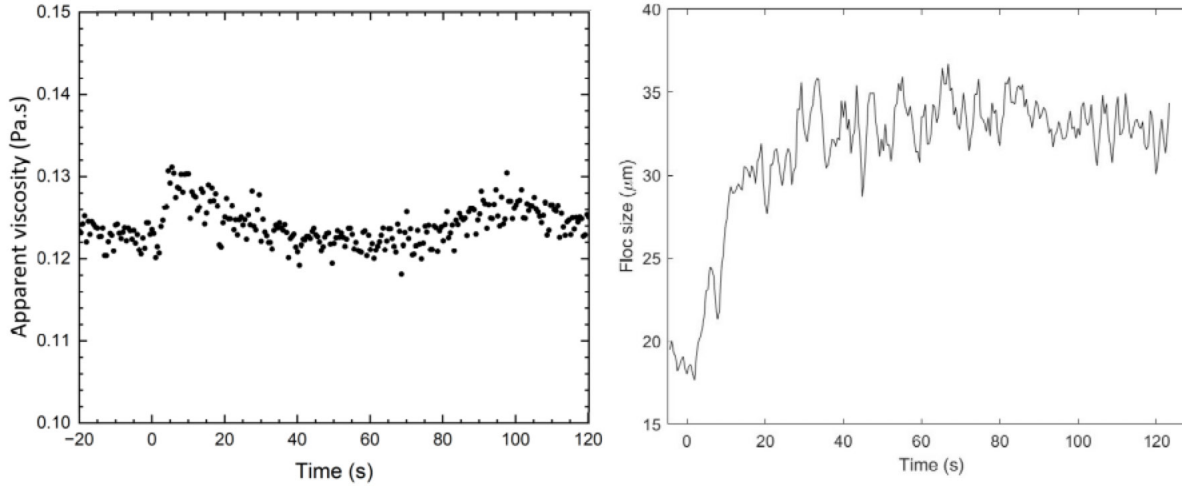

14. Flocculation and viscosity responses of 0.5% base paper stocks consisting of 20% BCTMP, 20% broke, and different amounts of HWBKP and SWBKP, with the dosage of cationic starch at 8 kg/metric ton: (a) Stock 1: 40% HWBKP and 20% SWBKP; (b) Stock 2: 50% HWBKP and 10% SWBKP; and (c) Stock 3: 60% HWBKP and 0% SWBKP.

a) Stock 4: BCTMP 20% + Broke 20% + HWBKP 55% + HRF 5% pre-treated with 40 kg/metric ton PAC

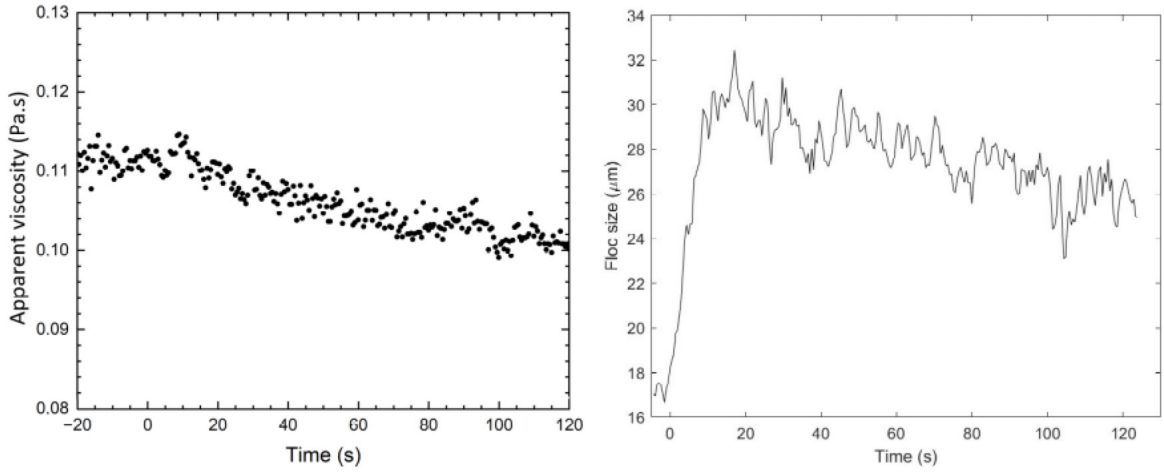

b) Stock 5: BCTMP 30% + Broke 20% + HWBKP 45% + HRF 5% pre-treated with 40 kg/metric ton PAC

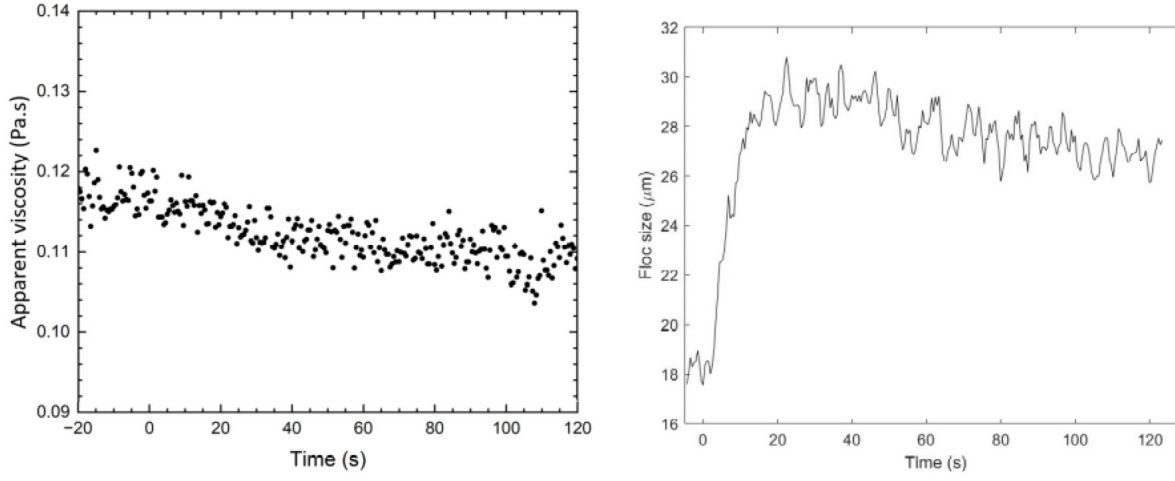

c) Stock 6: BCTMP 40% + Broke 20% + HWBKP 35% + HRF 5% pre-treated with 40 kg/metric ton PAC

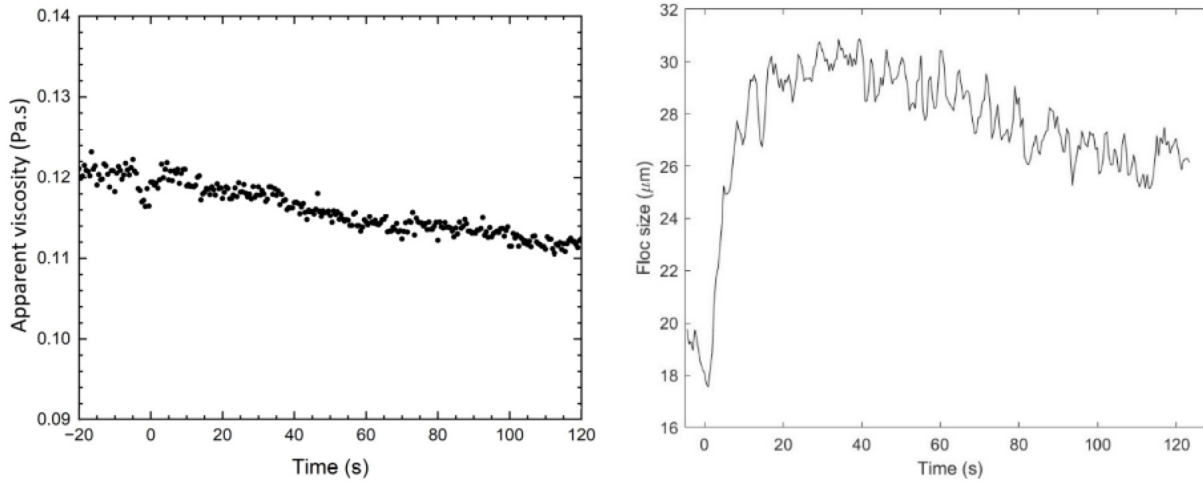

15. Flocculation and viscosity responses of 0.5% base paper stocks consisting of 20% broke, 5% HRF pretreated with PAC, and different amounts of HWBKP and BCTMP, with the dosage of PAC at 8 kg/metric ton: (a) Stock 4: 20% BCTMP and 55% HWBKP; (b) Stock 5: 30% BCTMP and 45% HWBKP; and (c) Stock 6: 40% BCTMP and 35% HWBKP.

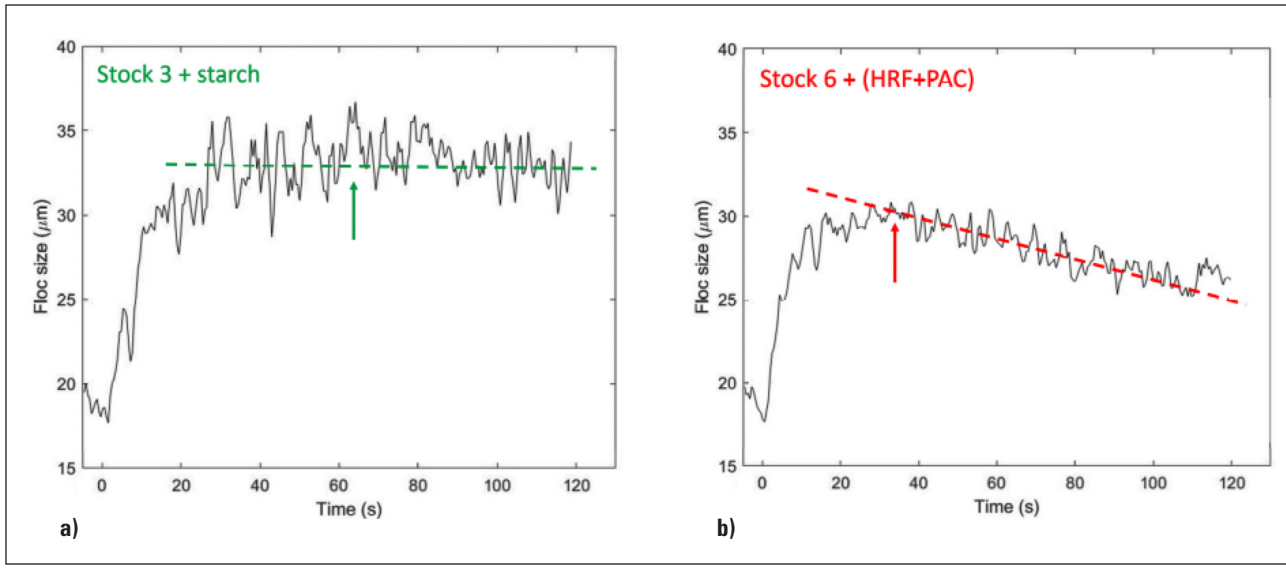

16. Flocculation dynamics comparison between the addition of (a) starch and (b) PAC treated HRF to the main stock. The arrows show the point in time of the highest floc size, and the dashed lines show the overall trend of the floc size after the addition of the additive.

CONCLUSIONS

In this work, we applied a novel method, Rheo-OCT, for the analysis of flocculation in papermaking stocks. Here, the viscosity of the fiber suspensions is measured with a rheometer, and the suspension floc structure is measured simultaneously with OCT. The advantages of OCT are the possibility to study opaque suspensions, its micron-level resolution, and its high data acquisition speed. We used Rheo-OCT to analyze, under constant shear, the time evolution of the floc size and the viscosity of the fiber suspension when the studied papermaking stocks were treated with highly refined furnish (HRF) and/or chemical additives. The measurements suggested that starch leads to larger flocs that can better resist shear forces than what is the case with the combination of HRF+PAC.

It is important to remember that in this study, the measurements were performed under a constant shear rate, while the actual papermaking process involves varying levels of shear forces at different stages. Nevertheless, this kind of study can lead to a better understanding of the impact of flocculation on the produced paper web, including its formation, drainage potential, and strength behavior.

In this work, the studied furnishes were intended for the filler ply of FBB. Typically, when fillers are applied in the filler ply, their amount is low compared to the outer plies and it is mainly carried by the broke. However, there is no fundamental reason that this measurement setup would not also work when fillers are included.

The presented approach of using less softwood, more mechanical furnish, HRF, and thus more fines for FBB filler ply, may offer potential reinforcement options, leading to bulk improvement and/or lower basis weight at similar internal bond levels. Here, a proposed approach to adding the HRF to the main stock is to first pretreat it with a flocculant (here PAC), and then add this mixture to the main stock rather close to the headbox to limit the time the formed flocs are under disruptive shear forces. **TJ**

ACKNOWLEDGEMENTS

The authors would like to thank Professor Martin A. Hubbe for his valuable discussions on polymer–HRF interactions, including complexation.

LITERATURE CITED

1. Blanco, A., Negro, C., and Tijero, J., *Developments in Flocculation: A Literature Review*, Pira International, Leatherhead, UK, 2001.
2. Kerekes, R.J. and Schell, C.J., *J. Pulp Pap. Sci.* 18(1): 32(1992).
3. Scott, W. E., *Principles of Wet End Chemistry*, TAPPI PRESS, Atlanta, 1996, Chap. 5, pp. 21-32.
4. Rasteiro, M. and Koponen, A., *Powders* 3(1): 77(2024). https://doi.org/10.3390/powders3010007.
5. Kellomäki, M., Karema, H., Kataja, M., et al., *Int. Pap. Physics Conf.*, TAPPI Press, Atlanta, 1999.
6. Karema, H., Salmela, J., Tukiainen, M., et al., "Prediction of paper formation by fluidisation and reflocculation experiments," in *The Science of Papermaking, Trans. of the XIIth Fund. Res. Symp., Oxford*, 2001 (C.F. Baker, Ed.), FRC, Manchester, 2018, pp. 559-589. https://doi.org/10.15376/frc.2001.1.559.
7. Blanco, A., Fuente, E., Negro, C., et al., *Can. J. Chem. Eng.* 80(4): 1(2002). https://doi.org/10.1002/cjce.5450800403.
8. Hubbe, M., *Emerging Technologies in Flocculation*, Pira International, Leatherhead, UK, 2005.
9. Gregory, J. and Nelson, D., *Colloids Surf.* 18(2-4): 175(1986). https://doi.org/10.1016/0166-6622(86)80312-2.

10. Burgess, M., Curley, J., Wiseman, N., et al., *J. Pulp Pap. Sci.* 28(10): 323(2002).

11. Anker, L., *TAPPI J.* 1(6): 3(2002).

12. Popescu, D., Choo-Smith, L.-P., Flueraru, C., et al., *Biophys. Rev.* 3(3): 15(2011). https://doi.org/10.1007/s12551-011-0054-7.

13. Koponen, A. and Haavisto, S., *KONA Powder Part. J.* 37: 42(2020). https://doi.org/10.14356/kona.2020003.

14. Koponen, A., Lauri, J., Haavisto, S., et al., *Appl. Sci.* 8(5): 75(2018). https://doi.org/10.3390/app8050755.

15. Lauri, J., Haavisto, S., Salmela, J., et al., *Cellulose* 28(6): 3373(2021). https://doi.org/10.1007/s10570-021-03745-6.

16. Haavisto, S., Salmela, J., Jäsberg, A., et al., *TAPPI J.* 14(5): 291(2015). https://doi.org/10.32964/10.32964/TJ14.5.291.

17. Mohtaschemi, M., Dimic-Misic, K., Puisto, A., et al., *Cellulose* 21: 1305(2014). https://doi.org/10.1007/s10570-014-0235-1.

18. Barnes, H.A. and Nguyen, Q.D., *J. Non-Newtonian Fluid Mech.* 98(1): 1(2001). https://doi.org/10.1016/S0377-0257(01)00095-7.

ABOUT THIS PAPER

Cite this article as:
Koponen, A.I., Cecchini, J., Laukkanen, O.-V., et al., *TAPPI J.* 23(9): 505(2024). https://doi.org/10.32964/TJ23.9.505

DOI: https://doi.org/10.32964/TJ23.9.505

ISSN: 0734-1415

Publisher: TAPPI Press

19. Owens, C.E., Hart A.J., and McKinley G.H., *J. Rheol.* 64(3): 643(2020). https://doi.org/10.1122/1.5132340.

ABOUT THE AUTHORS

Koponen

Cecchini

Laukkanen

Jäsberg

Papermakers are pressured to use more economical fibers and chemical additives while simultaneously achieving bulkier, stiffer, and stronger paperboard structures. Reaching this goal is not straightforward and requires extensive analysis to assess the potential of various approaches. A key factor in this process is understanding how fiber flocculation responds to chemical additives, as it influences how fibers interlock and form networks when creating a paper web.

In this paper, we presented a novel method, Rheo-OCT, for the simultaneous analysis of flocculation and rheological behavior in fiber suspensions. This approach provided novel insights, e.g., for the stock flocculation when highly refined furnish, pretreated with a flocculation additive, was used for reinforcement.

In the laboratory studies, it was initially unclear which shear rate to use for measurements. This issue was addressed by gradually increasing the shear rate and selecting the rate at which the floc size decreased during operation. The measurements were conducted under a constant shear rate, while the papermaking process involves varying shear forces at different stages. Therefore, the final validation will take place on an actual folding boxboard machine.

We discovered that the combination of multiple stocks and chemicals has not been extensively evaluated through rheology and flocculation analysis to identify potential improvements in board properties. Interestingly, it was possible to identify a combination of fiber types, refining methods, and inexpensive chemical additives that achieved paper properties similar to, or even better than, those obtained with more expensive combinations. Paper mills could potentially have cheaper alternatives to achieve similar strength while improving bulk and stiffness in their products.

Replacing bleached kraft pulp reinforcement fibers such as softwood with hardwood at the same refining level, and using polyaluminum chloride (PAC) instead of starch as additives, was a clear differentiator when increasing mechanical pulp content. In future research, we will examine whether or not similar results be achieved using only broke. While broke has been a common resource for paper and board makers for reinforcement, it is not always the most efficient. What would be required to effectively optimize the use of broke?

Koponen is principal scientist; Laukkanen is research scientist; and Jäsberg is senior scientist at VTT Technical Research Centre of Finland in Jyväskylä, Finland. Cecchini is senior development manager at Valmet Technologies in Jyväskylä, Finland. Email Koponen at Antti.Koponen@vtt.fi.

20. Chaparian, E., Owens, C.E., and McKinley, G.H., *J. Non-Newtonian Fluid Mech.* 307: 104857(2022). https://doi.org/10.1016/j.jnnfm.2022.104857.

21. Martínez-Padilla, L.P. and Quemada, D., *J. Food Eng.* 80(1): 24(2007). https://doi.org/10.1016/j.jfoodeng.2006.01.092.

22. Crawford, N., Sprague, M., and Stickel, J., *Chem. Eng. Sci.* 144: 310(2016). https://doi.org/10.1016/j.ces.2016.01.028.

23. Ovarlez, G., Mahaut, F., Bertrand, F., et al., *J. Rheol.* 55(2): 197(2011). https://doi.org/10.1122/1.3526349.

24. Hubbe, M., *BioResources* 1(2): 281(2006). https://doi.org/10.15376/biores.1.2.281-318.

25. Xiao, L., Salmi, J., Laine, J., et al., *Nord. Pulp Pap. Res. J.* 24(2): 148(2009). https://doi.org/10.3183/npprj-2009-24-02-p148-157.